On the radiative properties of soot aggregates part 2: effects of coating

Liu, Fengshan; Yon, Jérôme; Bescond, Alexandre

Publisher's version / Version de l'éditeur:
https://doi.org/10.1016/j.jqsrt.2015.08.005
Journal of quantitative spectroscopy and radiative transfer, 2015-08-20

On the radiative properties of soot aggregates part 2: effects of coating

Fengshan Liu[a*], Jérôme Yon[b], Alexandre Bescond[b]

[a]Black Carbon Metrology, Measurement Science and Standards, National Research Council, Ottawa, Ontario, Canada K1A 0R6

[b]CORIA-UMR6614, Normandie Université, CNRS, INSA et Université de Rouen, Av de l'Université, 76800 Saint Etienne du Rouvray, France

***Corresponding author**: Fengshan.Liu@nrc-cnrc.gc.ca

Abstract

The effects of weakly absorbing material coating on soot have attracted considerable research attention in recent years due to the significant influence of such coating on soot radiative properties and the large differences predicted by different numerical models. Soot aggregates were first numerically generated using the diffusion limited cluster aggregation algorithm to produce fractal aggregates formed by log-normally distributed polydisperse spherical primary particles in point-touch. These aggregates were then processed by adding a certain amount of primary particle overlapping and necking to simulate the soot morphology observed from transmission electron microscopy images. After this process, a layer of coating of different thicknesses was added to these more realistic soot aggregates. The radiative properties of these coated soot aggregates over the spectral range of 266 to 1064 nm were calculated by the discrete dipole approximation (DDA) using the spectrally dependent refractive index of soot for four aggregates containing N_p = 1, 20, 51 and 96 primary particles. The considered coating thicknesses range from 0% (no coating) up to 100% coating in terms of the primary particle diameter. Coating enhances both the particle absorption and scattering cross sections, with much stronger enhancement to the scattering one, as well as the asymmetry factor and the single scattering albedo. The absorption enhancement is stronger in the UV than in the visible and the near infrared. The simple corrections to the Rayleigh-Debye-Gans fractal aggregates theory for uncoated soot aggregates are found not working for coated soot aggregates. The core-shell model significantly overestimates the absorption enhancement by coating in the visible and the near

to significantly enhanced absorption cross section by up to about a factor of 2 [5,6,7], even though these coating materials are weakly- or even non-absorbing. This enhanced absorption due to coating is often referred to as the lensing effect [8,9,10].

Various mixing states between soot particle and other WAM aerosol compounds have been observed in the transmission electron microscopy (TEM) images of sampled aerosol particles [5,6]. It has been made clear that the internal mixing situation, where the soot aggregate is fully embedded by WAM, leads to the most enhancement in the coated particle absorption cross section [1,6] and has drawn much of the research attention recently.

In most climate models the radiative properties of soot aerosols are modelled using the Mie theory applied to either a core-shell system or a homogeneous sphere with the help of a mixing rule, such as the Maxwell-Garnet effective medium approximation [2,6]. Other extensions of the core-shell type model have been proposed and evaluated by Kahnert and co-workers [11,12]. In general, the performance of such simple mixing models is highly dependent on the mixing states of the coated soot particles [11,12]. For climate modelling the required radiative properties are the mass absorption cross section (MAC), single scattering albedo (SSA), and the asymmetry parameter (g) [6]. Although the Mie theory performs fairly well when the absorbing core is a spherical particle [13] or non-aggregated graphite particles [7] against experimentally measured absorption enhancement, it has been found to significantly overestimate the absorption enhancement in the visible spectrum [14]. The experimental measurements of atmospheric black carbon conducted by Cappa et al. [15,16] also showed that the measured absorption enhancement by WAM coating was much lower than that predicted by the core-shell Mie theory. These inconsistent findings suggest that the effects of WAM coating on soot aggregates deserve further research.

Although the radiative properties of uncoated or dry soot have been extensively studied by using the approximate Rayleigh-Debye-Gans theory for fractal aggregates (RDG-FA) [17-20] and several more advanced numerical methods, e.g. [21-26] among others. However, there have been fewer studies on the radiative properties of coated soot particles employing accurate numerical methods or dealing with realistic soot particle morphology and the mixing state. Due to the limitations of the T-matrix method [27] and the generalized Mie-solution method (GMM) [28], several studies had to use a simplified representation of the coating of WAM over a soot aggregate by an aggregate formed by individually coated primary particles [29-31]. Although

Kahnert et al. treated the soot aerosol particles as fairly compact fractal aggregates formed by monodisperse point-touch spherical primary particles with a fractal dimension of $D_f = 2.6$ and a prefactor of $k_f = 1.2$ and partially encapsulated the soot aggregates by a large spherical particle representing the host sulfate based on a typical morphology from TEM images [11]. To obtain the radiative properties of such complex shaped particles at three wavelengths (304, 533, and 1010 nm), Kahnert et al. used the DDSCAT code [34]. The accuracy of four simplified mixing models was evaluated against the DDSCAT results. In a follow up study, Kahnert et al. [12] employed the same methodology as in [11] to evaluate the accuracy of four simplified mixing models to approximate the partially encapsulated soot aggregates by sulfate concerning both climate- and remote sensing-relevant radiative properties. Soewono and Rogak [35] conducted a study of the optical properties of numerically generated fractal aggregates formed by monodisperse spherical primary particles (30 nm in diameter) in point-touch with and without a uniform layer of coating by non-absorbing material over the outer surface of aggregates. They applied the DDSCAT code (version 7.0) to calculate the optical properties at a wavelength of 532 nm. Most of the calculations were conducted for soot aggregates with $D_f = 1.78$ over the coating thickness range of 5 to 20 nm. They showed that the core-shell Mie model significantly underestimates the absorption cross sections of the coated soot particles, which had been observed by Khanert et al. [11]. Very recently, Dong et al. [36] investigated the effects of fractal dimension D_f in the range of 2.0 to 2.6 and aggregate size N_p (the number of primary particles) in the range of 50 to 600 on the radiative properties of soot aggregates in four mixing states (bare, partly coated, heavily coated, and with inclusion) at 550 nm using DDSCAT 7.3 [37]. The fractal soot aggregates formed by uniform primary particles in point-touch were generated using the tunable algorithm described by Skorupski et al. [38]. They also evaluated the accuracy of the homogeneous sphere model and the core-shell model.

It is noticed that all recent studies of the radiative properties of coated or internally mixed soot particles with WAM considered soot as fractal aggregates formed by monodisperse spherical primary particles in point-touch [11,12,29-32,35,36]. However, the TEM images of soot particles collected from either flames or engine exhausts reveal that primary particles are not in point-touch, but overlap each other and the contact areas between neighbouring primary particles display a smooth profile. The former is commonly known as overlapping and the latter as necking [36,37]. A numerical technique to add overlapping and necking to neighbouring

In this study, aggregates formed by polydisperse primary particles are generated by a diffusion limited cluster aggregation (DLCA) algorithm similar to that described by Hayashi et al. [44]. It is well known that DLCA fractal aggregates have a fractal dimension of about 1.8 [20]. To generate fractal aggregates with a higher fractal dimension to simulate the collapse of soot structure under heavy coating, the tunable algorithm developed by Skorupski et al. [38] can be used. The algorithms to add overlapping and necking between neighbouring primary particles described below can still be applied. In our DLCA generation of aggregates, the primary particles are polydisperse and follow a lognormal distribution with d_g = 26.6 nm and σ_g = 1.31, which are typical values of flame generated soot under the miniCAST 60/0/1.5/20 configuration. The simulation starts with unaggregated, i.e., isolated, primary particles with a prescribed particle volume fraction. With increasing time primary particles start to aggregate through the diffusion process to form increasingly large aggregates. Aggregates with sizes ranging from N_p = 1 to 500 (the number of primary particles in an aggregate) were generated in this study; however, DDA calculations were only conducted for N_p = 1, 20, 51 and 96. An analysis of the resultant aggregates showed that their fractal dimension and prefactor are 1.76 and 1.36, respectively.

2.2 Adding overlapping and necking

For a more realistic representation of dry soot aggregates, overlapping and necking between primary spheres need to be added to the DLCA aggregates, in which primary particles are in point-touch. For few selected aggregates generated in the first step described above, they were processed by introducing a certain degree of primary particle overlapping and necking. Overlapping and necking between neighbouring primary particles are schematically shown in Fig. 1. While overlapping reduces the total mass of an aggregate, necking increases the aggregate mass due to deposition of material in the contact region between neighbouring particle particles, Fig. 1(c). The definitions of overlapping and necking parameter, C_{ov} and α, respectively, follow those described by Bescond et al. [39] and Yon et al. [40]. As shown by Bescond et al. [39], C_{ov} = 0.2 and α = 0.5 best reproduce the TEM images and the experimentally observed depolarization of soot formed in an atmospheric laminar ethylene diffusion flame. These overlapping and necking parameters were also used in this study. Further details of adding overlapping and necking between neighbouring primary particles are given in [39,40].

coated aggregates generation are no longer identifiable as a result of overlapping and necking between neighbouring primary particles. The coating thickness at p = 100% is quite thick as shown in Fig. 2. As pointed out earlier, the potential collapse of the soot core into a more compact structure under heavy coating is not taken into account in this study.

[Insert Fig. 2 here]

The 3D levelset approach to add coating used in this study is a good choice to add relatively low level of coating and when the soot aggregate is nearly uniformly coated. To generate off-center coated soot particles or partially encapsulated soot particles, modifications to the present algorithm are necessary or other methods may be used, such as the method described by Dong et al. [36].

2.4 Morphology analysis

As shown in the first part of this study [40], overlapping and necking lead to the introduction of an equivalent number of primary spheres N_p^* of an aggregate, which is defined as the ratio of the mass of the core aggregate and the mass of the mean primary particle. Except for the case of only one sphere, the equivalent number of primary particles N_p^* for $C_{ov} = 0.2$ and $\alpha = 0.5$ is found to be larger than the initial aggregate size N_p (see Table 1).

The gyration radii, anisotropies, equivalent sphere radii and number of dipoles for the four selected aggregates with different levels of coating up to 100% are summarized in Table 1. Gyration radius and anisotropy are based on the eigenvalues of the matrix of inertia as outlined in Part 1 of the paper [37]. The bulk densities for the soot core and the coating material are assumed to be $\rho_{core} = 1543\ kg/m^3$ and $\rho_{coating} = 1227\ kg/m^3$, respective, corresponding to the density of soot particles generated by miniCAST for operating conditions associated with OC/TC ratios of 16 and 87% [45]. The volumes of the soot core and the coating are also reported in Table 1. The analysis of these volumes shows that the coating volume added to the particle relative to the volume of the core decreases with the number of primary spheres due to the increasing number of connections between spheres. Naturally, this percentage increase with the coating parameter p. For example, in the case of $N_p = 96$, the coating volume represents 37,

75	1	1	29.37	28.37	1.00	36.62	8217	1.30E+04	1.93E+05
75	20	31	28.70	71.53	1.76	83.68	105005	3.79E+05	2.08E+06
75	51	72	27.63	98.92	3.22	100.36	202395	7.95E+05	3.44E+06
75	96	133	27.77	138.61	4.32	120.82	349000	1.49E+06	5.90E+06
100	1	1	29.37	34.10	1.00	44.02	13997	1.30E+04	3.44E+05
100	20	31	28.70	79.51	1.59	95.88	157978	3.79E+05	3.31E+06
100	51	72	27.63	105.83	2.87	112.15	282391	7.95E+05	5.11E+06
100	96	133	27.77	144.40	3.99	134.03	476567	1.49E+06	8.60E+06

Coating fills the vacant spaces in the aggregate leading to an increase of its compactness. This is characterized by the increase in the slopes in the log-log fractal plot shown in Fig. 3. In this figure, we represent the total aggregate volume divided by the volume of the mean primary sphere as a function of the normalized particle gyration radius. We observe an increase in the fractal dimension (power-law) starting from $D_f = 1.76$ without any coating to $D_f = 2.14$ for the maximum considered coating thickness ($p = 100\%$). It is also observed that coating considerably increases the fractal prefactor (linked to the intercept with the vertical axis of the log-log plot).

3. Calculations of radiative properties

DDA was used in the present study due to its capability of handling complex shapes such as the coated soot particles shown in Fig. 2. Numerical calculations were conducted using the DDSCAT code version 7.3 [37] and using the wavelength dependent refractive index of soot over the spectral range of 266 to 1064 nm based on the following two considerations. First, the relevant wavelengths for solar radiation are in the range from 280 nm to past 2000 nm with the UV to near infrared range being the most important. Secondly, radiative properties of coated soot aggregates are required in optically based soot diagnostics, such as the laser-induced incandescence and light scattering techniques. The refractive indices used in our calculations were measured for soot produced by CAST generator under a condition of fairly high elemental carbon (96%) [40] are listed in Table 2. Also provided in Table 2 are the corresponding values of $E(m)$ and $F(m)$. The refractive index of the coating WAM is assumed independent of wavelength

criterion of $|m|kd < 0.5$ required for obtaining accurate absorption and differential scattering cross sections of tetrahedral [46],but also the more stringent criterion of $|m|kd < 0.32$ proposed by Kahnert et al. [11,12] for coated aggregates. DDSCAT calculations for the largest aggregate of $N_p = 96$ are very computationally intensive, especially for the largest coating thickness. For example, the 100% coating case took more than 8 days running the parallel version of DDSCAT with 16 CPUs on CRIHAN (for results at all the seven wavelengths). To evaluate the accuracy of the core-shell model of the Mie theory applied to the coated soot aggregates, this simplified and computationally very efficient model was also used in this study for the largest aggregate studied ($N_p = 96$). DDSCAT results for the largest aggregate considered are also compared to those of GMM for individually coated primary particles in point-touch.

4. Results and discussion

We first apply DDSCAT to calculate the radiative properties of a single coated spherical particle ($N_p = 1$) at 532 nm and compare the DDSCAT results with those of the core-shell Mie theory. The BHCOAT program [47] was used to conduct the core-shell Mie calculations. It was found that the relative errors of the absorption and scattering cross sections of DDSCAT at 532 nm remain below 3% and 1%, respectively. Similar levels of error of the DDSCAT results are also found at the other wavelengths investigated. This level of accuracy of DDSCAT is expected since the criterion of $|m|kd < 0.32$ recommended by Kahnert et al. [11,12] is satisfied. Then the radiative properties of coated soot calculated by DDSCAT are presented for the differential scattering, total scattering, and absorption cross sections following the same methodology as Part 1 of this study for the purpose of extending the RDG-FA theory to coated soot aggregates with the help of correction factors introduced in [40]. Finally, the DDSCAT results of the largest aggregate considered ($N_p = 96$) are compared with those of the core-shell Mie model and GMM for aggregates formed by individually coated primary particles.

4.1. Effects of WAM coating: DDSCAT results

[Insert Figure 4 here.]

In Fig. 4, the differential scattering cross sections are normalized by the respective value at the forward direction, which itself is also strongly affected by coating. To illustrate how coating affects the differential cross section in the forward direction as a function of the coating parameter for the 3 aggregates (N_p = 20, 51, and 96) at the 7 wavelengths, values of the A parameter defined as the ratio between the scattering cross sections in the forward direction and $C_{ve}{}^{p}N_{p}{}^{*2}$ are shown in Fig. 5. Note that the A parameter can be considered as a correction factor to the scattering cross section predicted by the RDG-FA theory [25, 40]. It is evident from Fig. 5 that coating enhances scattering in the forward direction and the enhancement increases significantly with the coating thickness and becomes weaker with increasing the aggregate size N_p at a given level of coating thickness, which is likely due to the decrease in the relative WAM volume with increasing N_p at a given coating thickness as discussed in Section 2.4. For example, at 100% coating and λ = 632 nm the correction to bring the RDG-FA theory for the forward scattering to the result of DDSCAT is about 35, 22 and 18 for increasing aggregate size N_p = 20, 51, and 97, respectively. Overall, the effect of wavelength is less important than the initial aggregate size and coating thickness. The maximum enhancement occurs at 632 nm in most cases. The results shown in Figs. 4 and 5 indicate that coating enhances the forward scattering and weakens the relative contribution of backward scattering (corresponding to the faster decay of the differential scattering cross section at large qR_g values in Fig. 4).

[Insert Fig. 5 here]

4.1.2 Total scattering

[40]. It is noticed that the horizontal axis of Fig. 7 is plotted in log scale due to the large variation of A for coated soot aggregates. However, such a simple linear relationship derived for uncoated soot aggregates in [40], i.e., $h = 1.11A$, can no longer be used to describe the $h \sim A$ relationship for coated soot aggregates, not even for thinly coated ones at $p = 10$ %. This behaviour is explained by the significantly more pronounced enhancement in scattering by the coating of WAM than the enhancement in absorption. In addition, the enhancement by coating in scattering and absorption has different spectral dependence. For absorption, the enhancement is stronger in the UV than in the visible and near infrared. However, for scattering the enhancement is weakly dependent on wavelength over the spectral range of 266 to 1064 nm. The DDSCAT results indicate that the absorption enhancement of coated soot aggregates is strongly dependent on the coating thickness and wavelength, but nearly independent of the size of the uncoated aggregates for $N_p = 20$ to 96 considered; however, the scattering enhancement is strongly dependent on all parameters (coating thickness, wavelength, and the size of uncoated aggregate N_p). This is perhaps why the simple linear relationship between h and A developed for uncoated soot aggregates cannot be observed for coated soot aggregates shown in Fig. 7. It is anticipated that the relationship between h and A is much more complex than a simple linear one and it is likely to be a function of the size and morphology of the uncoated soot aggregates, the coting thickness (or the soot core volume fraction of the coated soot particle), wavelength, and the refractive index of the coating material. Development of such a relationship will be the subject of a future study.

[Insert Fig. 7 here.]

4.1.3 Asymmetry factor and single scattering albedo

Besides the absorption and scattering cross sections, the asymmetry factor $\langle g \rangle$ and SSA are also important radiative properties for climate modelling. The effects of WAM coating on $\langle g \rangle$ and SSA are shown in Fig. 8 as a function of the size parameter of the coated aggregate for all 3 aggregates and 7 wavelengths considered. It is noticed that the gyration radii are provided in

4.2 Comparison between DDSCAT and core-shell Mie model results

Most climate models employ the Mie method to calculate the radiative properties of coated soot particles by approximating the particle as a concentric core-shell system or a homogeneous sphere with the help of a mixing rule, such as the Maxwell-Garnet effective medium approximation primarily due to the simplicity of such treatments [2]. It has been found in some studies that such simple models can be quite inaccurate, e.g. [11,14,15]. On the other hand, some other studies reached different conclusions, e.g. [7,13]. Therefore, it is useful to examine the accuracy of the core-shell model under the present conditions. Here the accuracy of the core-shell Mie model for treating the coated soot particles as a core-shell system is validated against the DDSCAT results. The Mie calculations were conducted using the BHCOAT code [47] and only for the largest aggregate size of N_p = 96. In the core-shell Mie calculations, the core diameter is determined in such a way that the soot core has the same volume as the soot aggregate and the shell thickness is chosen to yield the same WAM coating volume as the actual one.

The absorption enhancement factors for different levels of coating from the Mie method are compared to those from the DDSCAT in Fig. 9. The absorption enhancement factor is defined as the ratio of the absorption cross section of the coated soot particle to that of the uncoated soot core from the same method. It is evident from Fig. 9 that the core-shell Mie model leads to significant overestimation of the absorption enhancement by WAM coating to soot aggregates, especially at longer wavelengths above about 500 nm, indicating that, even in the near IR, the specific morphology of aggregates should be taken into account in the prediction of absorption enhancement by WAM coating. These results are in qualitative agreement with the observations of Kahnert et al. [11] and Soewono and Rogak [35]. Under the present conditions the absorption enhancement factors are up to about 1.5 in the UV and less than 1.25 in the near IR for DDSCAT and up to about 1.35 in the UV and about 1.6 in the visible and the near IR for the core-shell Mie model.

[Insert Fig. 9 here]

is the radius of the ith primary particle and q is a parameter which is determined in such a way that the total coating volume is the same as that in the coated soot aggregate. Correspondingly, the centre of coated primary particles is also expanded so that the coated primary particles are still in point-touch.

A direct comparison between the absorption cross sections of the coated soot aggregate calculated by DDSCAT and those of an aggregate formed by individually coated primary particles in point-touch calculated by GMM is provided in Fig. 11. It is observed that in the case of no coating the DDSCAT results are in good agreement with those of GMM. This also provides validation of the DDSCAT results since in this case the GMM results are considered numerically exact. When coating is added to the aggregate, except at 266 nm, where the individually coated primary particles model overpredicts the absorption cross section, the individually coated primary particles mixing model in general significantly underpredicts the absorption cross section of the coated soot aggregate at longer wavelengths. In addition, treating the externally coated soot aggregate as individually coated primary particles significantly underestimates the enhancement in absorption by WAM coating in the visible and the near IR spectrum. Such a comparison helps understand how realistic it is to treat a coated soot aggregate as an aggregate formed by individually coated primary particles, which has been used in several previous studies [29-31].

[Insert Fig. 11 here]

5. Conclusions

More realistic soot aggregates were generated in this study to better represent the soot morphology observed from TEM images of sampled flame generated soot particles. Specifically, the generation algorithm takes into account the polydisperisty, overlapping, and necking of primary particles. Using these more realistic numerical soot aggregates as the core of coated soot particles, the present study investigated the effects of WAM coating on the radiative properties of soot particles over the spectral range of 266 to 1064 nm using DDSCAT for coating thickness up to the primary particle diameter or the ratio of the volume equivalent diameter of the coated particle to that of the core up to about 2.

models for efficient and reasonably accurate calculations of the radiative properties of coated soot particles.

Acknowledgements

The authors thank the CRIHAN for the computational resources provided by the Haute-Normandie region and the University of Rouen for its financial support. Fengshan Liu would like to thank the financial support by NRCan PERD AFTER Project C23.006 and Jérôme Yon would like to thank the French Carnot Institute Energy and Propulsion Systems (ESP) for their financial support. We also thank Professors B.T. Draine and P.J. Flatau for making DDSCAT 7.3 program available.

References

1. Jacobson MZ. Strong radiative heating due to the mixing state of black carbon in atmospheric aerosols. Nature 2001;409: 695-697.
2. Bond TC, Doherty SJ, Fahey DW et al. Bounding the role of black carbon in the climate system: a scientific assessment. J Geophys. Res. 2013;118:5380-5552.

14. Adachi K, Chung SH, Buseck PR. Shapes of soot aerosol particles and implications for their effects on climate. J Geophys. Res. 2010;115, D15206, doi:10.1029/2009JD012868.
15. Cappa CD, Onasch TB, Massoli P, et al. Radiative absorption enhancements due to mixing state of atmospheric black carbon. Science 2012;337:1078-1081.
16. Cappa CD, Onasch TB, Massoli P, et al. Response to comment on "radiative absorption enhancements due to mixing state of atmospheric black carbon". Science 2013;339:393-c.
17. Dobbins RA, Megaridis CM. Absorption and scattering of light by polydisperse aggregates. Appl. Opt. 1991;30(33):4747–54.
18. Farias TL, Carvalho MG, Köylü ÜÖ, Faeth GM. Computational evaluation of approximate Rayleigh-Debyre-Gans/fractal-aggregate theory for the absorption and scattering properties of soot. ASME J Heat Transfer 1995;117:1520159.
19. Farias TL, Köylü ÜÖ, Carvalho MG. Range of validity of the Rayleigh-Debye-Gans theory for optics of fractal aggregates. Appl. Optics 1996;35:6560-6567.
20. Sorensen CM. Light scattering by fractal aggregates: a review. Aerosol Sci. Tech. 2001;35:648-687.
21. Mulholland GW, Bohren, CF, Fuller KA. Light scattering by agglomerates: coupled electric and magnetic dipole method. Langmuir 1994;10:2533–2546.
22. Liu L, Mishchenko MI. Effects of aggregation on scattering and radiative properties of soot aerosols. J Geophys. Res. 2005;110, D11211, doi:10.1029/2004JD005649.
23. Liu L, Mishchenko MI, Arnott WP. A study of radiative properties of fractal soot aggregates using the superposition T-matrix method. J Quant Spectrosc Radiat Transfer 2008;109:2656–2663.
24. Liu F, Smallwood GJ. Radiative properties of numerically generated fractal soot aggregates: the importance of configuration averaging. ASME J Heat Transfer 2010;132:023308-1–023308-6.
25. Yon J, Liu F., Bescond A, Caumont-Prim C, Rozé C, Ouf F, Coppalle A. Effects of multiple scattering on radiative properties of soot fractal aggregates. J Quant Spectrosc Radiat Transfer 2014;133:374-381.

38. Skorupski K, Mroczka J, Wriedt T, Riefler N. A fast and accurate implementation of tunable algorithms used for generation of fractal-like aggregate models. Physica A: Stat Mech Appl 2014;404:106-117.
39. Bescond A, Yon J, Girasole T, Jouen C, Rozé C, Coppalle A. Numerical investigation of the possibility to determine the primary particle size of fractal aggregates by measuring light depolarization. J Quant Spectrosc Radiat Transfer 2013;126:130-139.
40. Yon J, Bescond A, Liu F. On the radiative properties of soot aggregates part 1 : Necking and overlapping. J Quant Spectrosc Radiat Transfer, in press, 2015.

41. Slowik JG, Cross ES, Han JH, Kolucki J, Davidovits P, Williams LR, Onasch TB, Jayne JT, Kolb CE, Worsnop DR. Aerosol Sci. Tech. 2007;41:734-750.
42. Khalizov AF, Xue H, Wang L, Zheng J, Zhang R. Enhanced light absorption and scattering by carbon soot aerosol internally mixed with sulfuric acid. J Phys. Chem. A 2009;113(6):1066-1074.
43. Ghazi R, Olfert JS. Coating mass dependence of soot aggregate restructuring due to coatings of oleic acid and dioctyl sebacate. Aerosol Sci. Tech. 2013;47:192-200.
44. Hayashi S, Hisaeda Y, Asakuma Y, Aoki H, Miura T, Yano H, Sawa Y. Simulation of soot aggregates formed by benzene pyrolysis. Combust. Flame 1999;117:851-860.
45. Yon J. Bescond A, Ouf FX. A simple semi-empirical model for effective density measurements of fractal aggregates. J Aersol Sci. 2015;87:28-37.
46. Draine, BT., The discrete dipole approximation for light scattering by irregular targets. In M.I. Mishchenko, J.W. Hovenier, L.D. Travis, eds. "Light Scattering by Nonspherical Particles: Theory, Measurements, and Application", pp. 131-145, 2000. San Diego: Academic Press.
47. Craig F. Bohren, Donald R. Huffman, Absorption and Scattering of Light by Small Particles. John Wiley & Sons, New York, 1983.

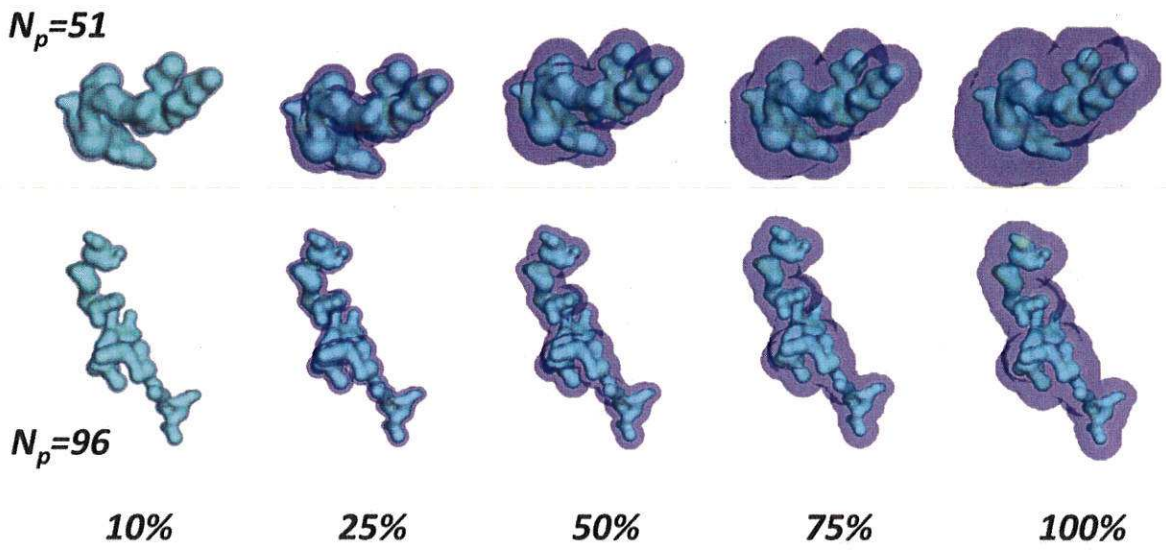

Fig. 2 Graphical illustration of the two largest soot aggregates investigated in this study at different levels of coating thickness from 10 to 100% of the primary particle diameter.

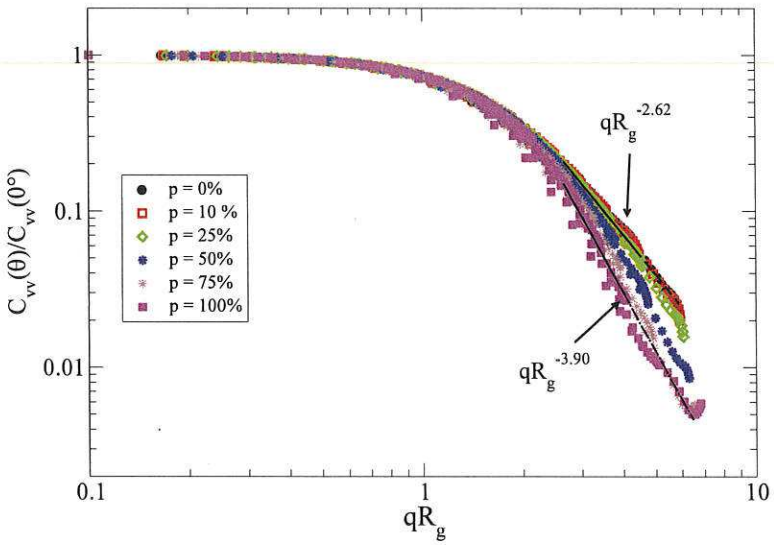

Fig. 4 Impact of coating on the normalized vertical-vertical differential scattering cross section (structure factor) for the largest aggregate (N_p = 96) considered. Results at all the seven wavelengths investigated are included.

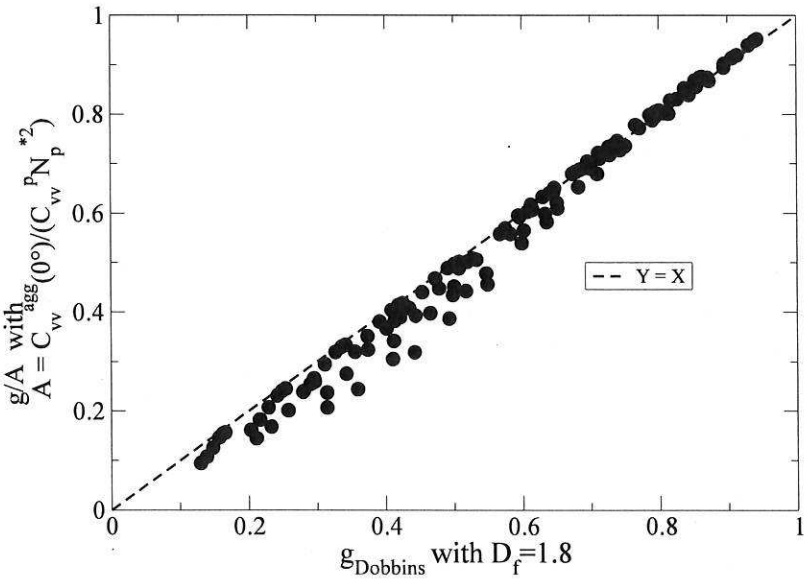

Fig. 6 The correlation between the multiple scattering effect corrected total scattering g function based on the DDA results with the RDG-FA g function for $D_f = 1.8$.

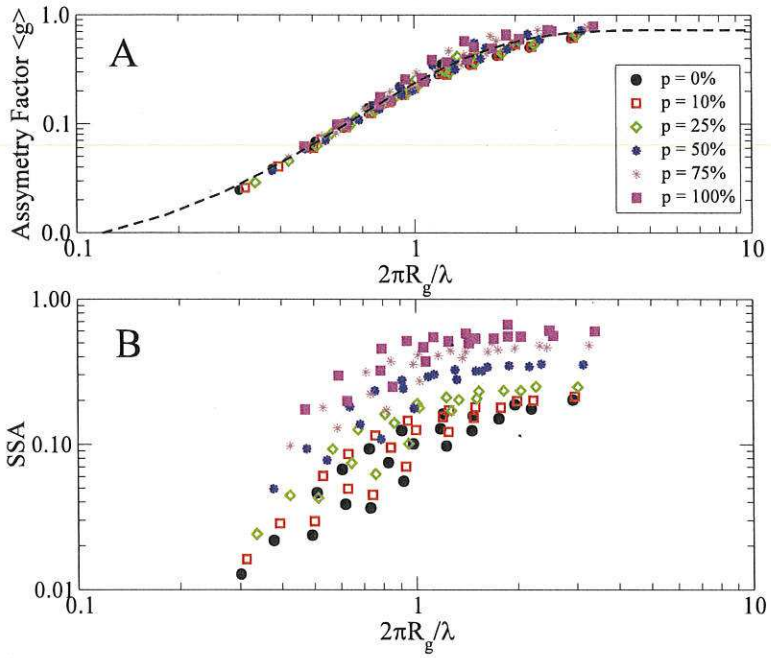

Fig. 8 Impact of the coating on the asymmetry factor, (a), and the single scattering albedo (SSA), (b), of coated soot aggregates as a function of the size parameter of the uncoated aggregates for all 3 considered aggregates and 7 wavelengths.

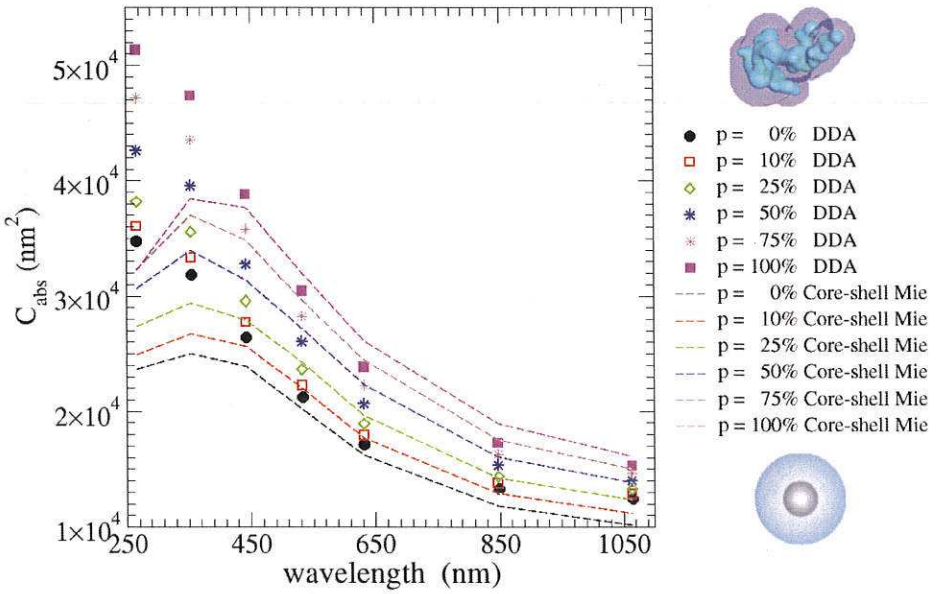

Fig. 10 Comparison of the absorption cross sections predicted by DDA and core-shell Mie at coating levels of 0 from to 100% for $N_p = 96$.